Mon. Not. R. Astron. Soc. **352,** 277–284 (2004) doi:10.1111/j.1365-2966.2004.07919.x

Is the slope of the intrinsic Baldwin effect constant?

M. R. Goad,[1]★ K. T. Korista[2] and C. Knigge[1]

[1]*School of Physics & Astronomy, University of Southampton, Highfield, Southampton SO17 1BJ*
[2]*Department of Physics, Western Michigan University, Kalamazoo, MI 49008-5252, USA*

Accepted 2004 April 13. Received 2004 April 8; in original form 2004 February 17

ABSTRACT

We investigate the relationship between emission-line strength and continuum luminosity in the best-studied nearby Seyfert 1 galaxy NGC 5548. Our analysis of 13 yr of ground-based optical monitoring data reveals significant year-to-year variations in the observed Hβ emission-line response in this source. More specifically, we confirm the result of Gilbert & Peterson of a non-linear relationship between the continuum and Hβ emission-line fluxes. Furthermore, we show that the slope of this relation is not constant, but rather decreases as the continuum flux increases. Both effects are consistent with photoionization model predictions of a luminosity-dependent response in this line.

Key words: methods: data analysis – galaxies: active – galaxies: Seyfert.

1 INTRODUCTION

Observations of correlated continuum and broad emission-line variations in active galactic nuclei (AGN) provide powerful diagnostics of the structure and physical conditions within the spatially unresolved broad emission-line region (BLR) and of the origin and shape of the unobservable ionizing continuum.

A well-established correlation is the observed decrease in broad emission-line equivalent width with increasing continuum level for AGN spanning a broad range in continuum luminosity; this is the so-called global 'Baldwin effect' (Baldwin 1977; Osmer, Porter & Green 1994). Originally observed in the strongest UV resonance lines (e.g. C IVλ1549 and Lyα), a global Baldwin effect has now been found for most of the strong UV emission lines. Interestingly, evidence for a similar effect in the broad optical hydrogen recombination lines remains weak.

In a recent study of composite quasar spectra spanning a broad range in continuum luminosity and redshift, Dietrich et al. (2003) found no evidence for evolution of the Baldwin effect with cosmic time. Instead, they suggested that the effect is a consequence of luminosity-dependent spectral variations, in the sense that the ionizing continuum becomes softer for higher continuum luminosities. This agrees well with the theoretical work by Korista, Baldwin & Ferland (1998), who showed that if the gas metallicity and continuum spectral energy distribution are related statistically to the quasar luminosity, then so will the emission-line equivalent widths, in a manner described by the Baldwin effect.

Formally, the relationship between the continuum luminosity $L_{\rm cont}$ and the broad emission-line luminosity $L_{\rm line}$ may be represented by a single power law, such that

$$L_{\rm line} \propto L_{\rm cont}^{\alpha}. \quad (1)$$

In terms of the line equivalent width $\mathrm{EW}_{\rm line}$, the Baldwin relation is then given by

$$\mathrm{EW}_{\rm line} \propto L_{\rm cont}^{\beta}, \quad (2)$$

where $\beta = \alpha - 1$. The measured values of α are typically <1, for example, $\alpha \approx 0.83$ for C IV and $\alpha \approx 0.88$ for Lyα (see, for example, Kinney, Rivolo & Koratkar 1990; Pogge & Peterson 1992), with corresponding slopes for the Baldwin relation of $\beta = -0.17$ and $\beta = -0.12$, respectively.

Superposed on the global Baldwin relation is a second relation, the slope of which reflects the emission-line response to variations in the ionizing continuum within an individual source. Now commonly referred to as the 'intrinsic Baldwin effect', this phenomenon accounts for at least some of the scatter seen in the global Baldwin relation. However, the intrinsic Baldwin relation also shows considerable scatter, the origin of which is largely attributable to continuum–emission-line time-delay effects (reverberation) within the physically extended broad emission-line region (see, for example, Krolik et al. 1991; Pogge & Peterson 1992; Peterson et al. 2002).

Formally, the relationship between the continuum flux $F_{\rm cont}$ and emission-line flux $F_{\rm line}$ within a single source can also be represented by a single power law, such that

$$F_{\rm line} \propto F_{\rm cont}^{\alpha}, \quad (3)$$

where, in this case, α is a measure of the instantaneous emission-line response to changes in the ionizing continuum flux – the *responsivity* of the gas. In terms of the line equivalent width, the intrinsic Baldwin relation is then given by

$$\mathrm{EW}_{\rm line} \propto F_{\rm cont}^{\beta}. \quad (4)$$

where again $\beta = \alpha - 1$.

★E-mail: mrg@astro.soton.ac.uk

Although a global Baldwin relation has yet to be seen in the optical recombination lines, there is no physical reason why an individual source should not display an intrinsic Baldwin effect in these lines. That is to say, the broad range in physical conditions extant within the BLR are such that case B recombination, for which $\alpha \equiv 1$, does not apply. Indeed, Gilbert & Peterson (2003) recently reported just such an effect for the broad Hβ emission-line in a comprehensive study of 10 yr of ground-based optical monitoring data on the nearby Seyfert 1 galaxy NGC 5548, taken as part of the AGNWatch collaboration. Interestingly, Gilbert & Peterson noted (their fig. 4) that, during a low-continuum-flux state (year 4 of the monitoring campaign), the relationship between the continuum and Hβ emission-line flux appeared to change. However, because there was only *one* low-flux state, they were unable to determine whether this change was a result of flux-dependent effects (e.g. photoionization) or time-dependent effects (e.g. a renormalization of the intrinsic relation due to a change in composition and/or distribution of the line-emitting gas).

Although variations in the emission-line response with continuum state have long been predicted by photoionization calculations (e.g. Goad 1995; O'Brien, Goad & Gondhalekar 1995; Korista & Goad 2004), they have so far never been reported in the observations. Here, we take a detailed look at all 13 yr of optical-continuum and emission-line data available for NGC 5548, including two new low-flux states. Using this unique data set, we have found the first observational evidence for luminosity-dependent variations in the emission-line response. These luminosity-dependent variations are not only apparent in the whole data set (reinforced by the addition of new low-continuum-flux data from years 12 and 13), but are even visible within individual observing seasons, being particularly prominent during those seasons displaying both high and low-continuum-flux states (e.g. year 4; see Section 3). Because the observed variations can occur on time-scales of less than 1 yr, they most likely represent a response to luminosity variations rather than to structural changes in the emission-line region.

2 13 YR OF OPTICAL DATA

The bright [$\lambda L(\lambda 5100\ \text{Å}) \sim 10^{43.5}$ erg s^{-1}], nearby ($z = 0.017$), Seyfert 1 galaxy NGC 5548 is perhaps the best-studied of all AGN at optical wavelengths. This galaxy has been the subject of a concerted monitoring campaign by the AGNWatch collaboration since 1990, having been observed over 1500 times with a mean sampling interval of $\sim$3 d (see, for example, Peterson et al. 2002, for a comprehensive review).

Here we analyse the optical-continuum and Hβ emission-line data for NGC 5548 in order to determine whether the Hβ emission-line response for this source is sensitive to the continuum level throughout the 13-yr duration of this campaign. For homogeneity, we use only data taken with the Ohio State CCD spectrograph on the 1.8-m Perkins Telescope at the Lowell Observatory in Flagstaff, Arizona. For a detailed review of the reduction procedure, we refer the reader to Peterson et al. (2002) and references therein. In brief, the continuum flux was measured in a 10-Å-wide bin centred at λ5100 Å in the rest frame of the galaxy. The Hβ emission-line flux was then determined by integrating the flux over a linear fit to the background continuum between λ4710 Å and λ5100 Å again in the rest frame of the galaxy. Fig. 1 shows the full 13 yr of continuum and line-flux measurements (observed frame) taken as part of the AGNWatch campaign.

2.1 Background removal

Both continuum and emission-line fluxes are contaminated by nuisance background components which must be removed. The continuum flux measurements are contaminated by a constant background contribution by starlight from the host galaxy. In addition, the broad Hβ emission-line flux is contaminated by a non-variable narrow-line component. For each component, we adopt the canonical values used by Gilbert & Peterson (2003) in their fit to the first 10 yr of the AGNWatch data, i.e. $F_{\rm galaxy} = 3.37 \pm 0.54 \times 10^{-15}$ erg cm^{-2} s^{-1} Å^{-1} for the continuum flux (Romanishin et al. 1995) and $F(\text{H}\beta_{\rm narrow}) = 6.7 \pm 0.6 \times 10^{-14}$ erg cm^{-2} s^{-1}.

2.2 Delay removal and error estimates from structure function analysis

The continuum and Hβ light curves are highly correlated, but the emission-line variations are delayed with respect to the continuum (Fig. 1). Physically, these delays arise because the continuum is produced close to the central engine of an AGN, whereas the line-forming region is located at larger distances, in the spatially extended BLR. Given that the line emission is ultimately powered by the continuum incident on the BLR, the lines thus respond to changes in the continuum with a time delay, τ, that is a measure of the luminosity-weighted radius, $R_{\rm BLR}$, of the BLR, i.e. $\tau \simeq R_{\rm BLR}/c$.

When determining emission-line responsivities, these delays are contaminants and must be corrected for. This is because the line responsivity is defined as the instantaneous emission-line response to short-time-scale small amplitude changes in the continuum flux incident on the BLR at the same time, i.e. $\alpha = \mathrm{d}\log F_{\rm line}/\mathrm{d}\log F_{\rm cont}$. In practice, we therefore shift the emission-line data for each year by their respective delays (as calculated from the centroids of the cross-correlation function for each of the 13 yr of data; see, for example, Peterson et al. 2002). We then estimate the continuum flux at each (shifted) emission-line epoch as the weighted average of the two bracketing continuum points.

The appropriate weight for each point is calculated from the first-order structure function derived from the continuum light curve. Detailed descriptions of structure function analysis may be found in Kawaguchi et al. (1998) or Paltani (1999) and references therein. Briefly, the first order structure function for a series of flux measurements $f(t_i)$, $i = 1, \ldots, N$, is defined as

$$S(\tau) = \frac{1}{N(\tau)} \sum_{i<j} [f(t_i) - f(t_j)]^2, \tag{5}$$

where the sum is over all pairs of points for which $t_j - t_i = \tau$, and $N(\tau)$ is the total number of pairs of points. It is straightforward to show that $S(\tau)$ is a measure of (twice) the variance of the light curve on time-scale τ, i.e. $S(\tau) \simeq 2\sigma^2(\tau)$. Correspondingly, structure functions are usually characterized by two flat sections with amplitudes of twice the total variance of the data, $2\sigma^2$, on the longest time-scales and twice the noise variance due to observational errors, $2\sigma^2_{\rm noise}$, on the shortest time-scales. These flat sections are typically joined by by a rising power law on intermediate time-scales.

Fig. 2 shows the structure functions for both the continuum (upper curve) and emission-line (lower curve) light curves for time-scales of <500 d. Given a pair of continuum points, the continuum structure function tells us immediately the correct weight to assign to each point in estimating the continuum flux at any time, t, between them. More specifically, each of the two points bracketing t is assigned the usual inverse variance weight $2/S(\tau) \simeq 1/\sigma^2(\tau)$, where $\tau = t_i - t$ and t_i is the time associated with each point.

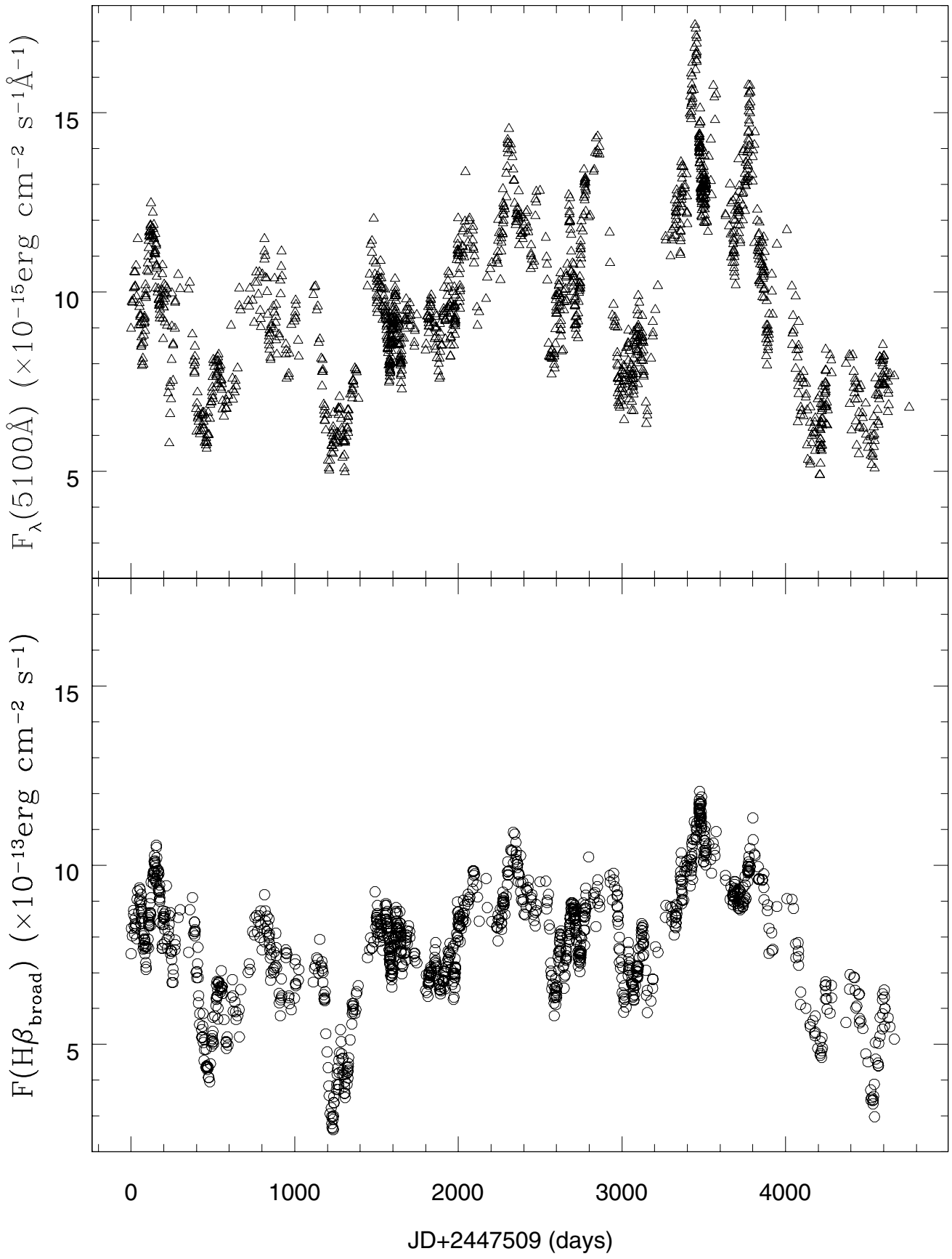

Figure 1. Upper panel $F(\lambda 5100$ Å) continuum light curve (observed frame) for the full 13-yr AGNWatch monitoring campaign of NGC 5548. Lower panel: the corresponding Hβ emission-line light curve.

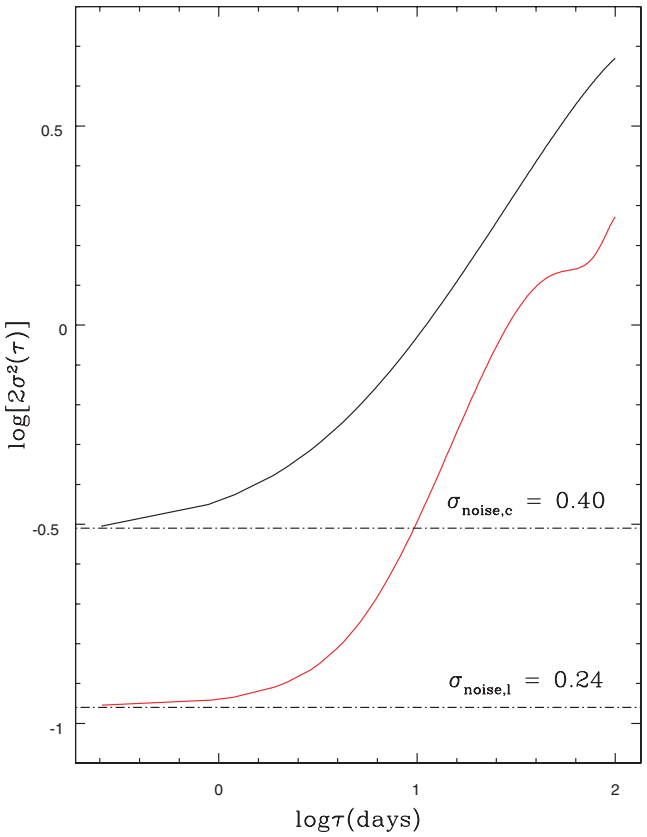

Figure 2. Computed structure functions for the continuum (upper curve) and Hβ light curves. Dot–dashed lines indicate the noise level in each of the light curves.

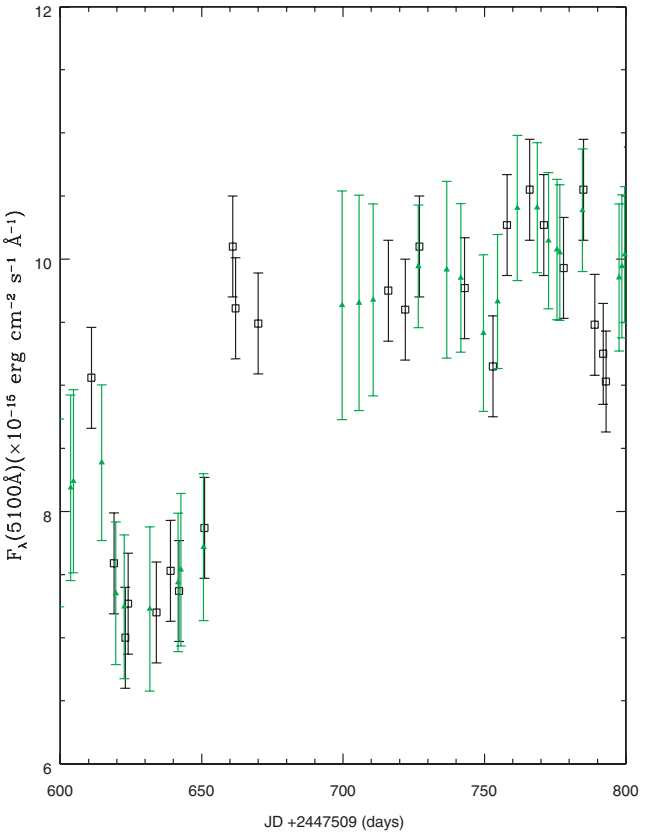

Figure 3. A section of the original continuum light curve (open squares) and the reconstructed continuum flux points (filled triangles), together with their associated uncertainties.

We also use the structure functions to estimate the errors on both emission-line and continuum flux estimates. Fig. 2 shows that the structure functions are flat on the shortest time-scales ($\tau \lesssim 1$ d). The corresponding estimates of the instrumental uncertainties are $\sigma_{\rm noise,c} = 0.4 \times 10^{-15}$ erg cm^{-2} s^{-1} Å^{-1} for the continuum and $\sigma_{\rm noise,l} = 0.24 \times 10^{-13}$ erg cm^{-2} s^{-1} for the line. Respectively, these correspond to fractional errors of $\sim$3 and $\sim$2 per cent at high continuum and line-flux levels, rising to $\sim$25 and $\sim$15 per cent at low continuum and line-flux levels. Because shifting the line data points leaves their flux values unaltered, we simply take the error on the line fluxes to be $\sigma_l = \sigma_{\rm noise,l}$. By contrast, the reconstructed continuum points are two-point weighted averages of the bracketing data values. We therefore assign errors corresponding to the standard deviation estimated from these data values,

$$\sigma_{\rm c}^2 = \frac{2}{\sum_{i=1}^{2} \frac{1}{\sigma_{(\tau_i)^2}}}. \qquad (6)$$

The factor 2 in the numerator is needed because we want the standard deviation of the two bracketing points, not the error on the mean. This ensures that the minimum error associated with a reconstructed point is $\sigma_{\rm noise,c}$ (rather than $\sigma_{\rm noise,c}/\sqrt{2}$).

Fig. 3 shows the input continuum (open squares), reconstructed continuum (filled triangles) and their associated errors for a small section of the 13-yr light curve. Note that in filling data gaps of less than a day, our reconstruction assigns uncertainties comparable to those on the original data points (i.e. $\sigma_{\rm noise,c}$). Where gaps are longer (e.g. boundaries between observing seasons), the uncertainties on the reconstructed points in the gaps increase with increasing distance from the nearest bracketing point. Both types of limiting behaviour are sensible.

3 RESULTS

Fig. 4 (upper panel) shows the λ5100 Å continuum flux versus Hβ emission-line flux after correcting for contaminating background components and the yearly continuum-emission-line time delays. Also shown (dashed line) is a linear least-squares fit to the data accounting for errors in both coordinates, and assuming that the data follow the relation

$$\log F({\rm H}\beta_{\rm broad}) = \log A + \alpha \log[F_\lambda(5100\,{\rm \AA}) - F_{\rm galaxy}]. \qquad (7)$$

The best-fitting slope α and 1σ uncertainty (estimated using bootstrap re-sampling), together with the mean continuum flux (unweighted) and rms error, are given in Table 1. Our estimated slope and 1σ uncertainty for the 13-yr campaign, 0.621 ± 0.019 (Table 1), is marginally smaller (but still within the estimated uncertainties) than that found by Gilbert & Peterson (2003) for the first 10 yr of data. We therefore confirm Gilbert and Peterson's finding of an intrinsic Baldwin effect for this line with slope $\beta \approx -0.4$.

The lower panel of Fig. 4 shows the same relation plotted against the binned continuum data. The continuum data were binned in 0.25-unit intervals in continuum flux with individual points in each bin weighted according to the uncertainties on the reconstructed continuum flux. The binned continuum data indicate evidence not only for a steepening of the observed relation at low-continuum-flux levels,

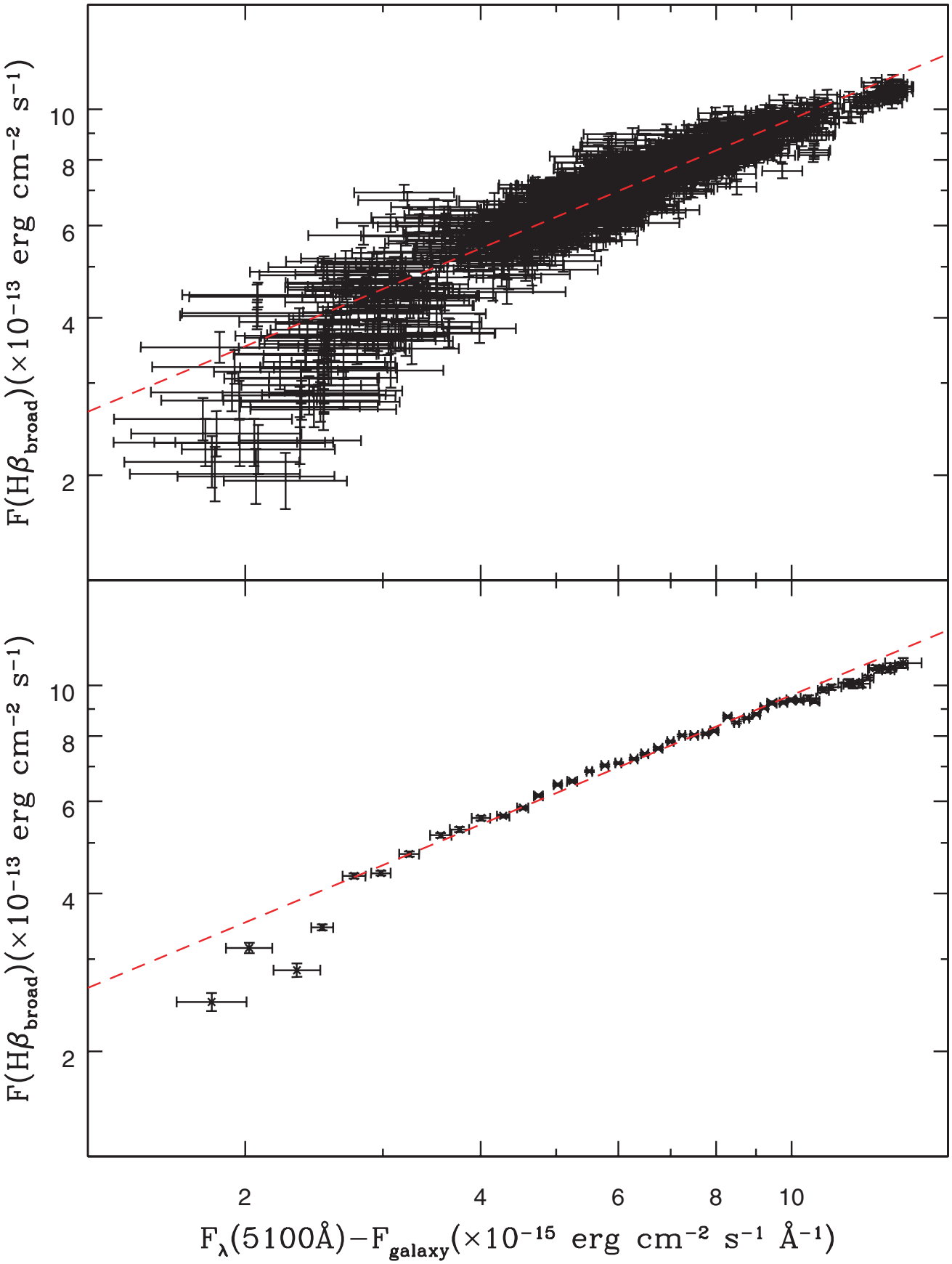

Figure 4. Upper panel: best-fitting slope (dashed line) to the full 13 yr of optical data. Lower panel: as above, only this time we show the data binned in 0.25 intervals in continuum flux (see text for details).

Table 1. The measured Hβ emission-line responsivities, α, and their 1σ uncertainties for combined and yearly data sets. Also shown are the corresponding values for the intrinsic Baldwin relation β. Quoted flux values are the unweighted means and rms error in units of 10^{-15} erg cm^{-2} s^{-1} Å^{-1}.

Year	α	$\beta = \alpha - 1$	σ_α σ_β	$\langle F_{\rm cont}\rangle$ ($\times 10^{-15}$)	$\sigma_{\langle F_{\rm cont}\rangle}$
All years	0.621	−0.379	0.019	6.33	2.41
1	0.558	−0.442	0.041	6.54	1.27
2	0.836	−0.164	0.034	3.79	0.91
3	0.946	−0.054	0.089	6.06	0.92
4	0.936	−0.064	0.050	3.34	1.17
5	0.430	−0.570	0.035	5.69	0.87
6	0.736	−0.264	0.040	6.40	1.11
7	0.677	−0.323	0.042	8.71	1.01
8	0.540	−0.460	0.028	7.07	1.52
9	0.800	−0.200	0.070	4.73	0.89
10	0.514	−0.486	0.021	10.05	1.44
11	0.410	−0.590	0.041	8.48	1.82
12	0.646	−0.354	0.060	3.59	1.20
13	1.000	0.000	0.116	3.65	0.86

as previously noted by Gilbert & Peterson (2003), but also for a flattening of the relation at the highest continuum fluxes.

In order to discriminate between temporal changes in the structure of the BLR and a luminosity-dependent emission-line response, we have also applied the same fitting routine to each year of data separately. Fig. 5 shows the best-fitting slopes (solid lines) for each of the 13 yr of data. To guide the eye, we also show the best-fitting slope (dashed line) determined for the full 13-yr campaign. The measured slopes and their 1σ uncertainties (again determined using bootstrap re-sampling) are given in Table 1.

4 DISCUSSION

Fig. 5 and Table 1 demonstrate that the Hβ emission-line responsivity, α, shows significant variations from one observing season to the next. To quantify this further, we show in Fig. 6 the mean continuum flux for each observing season versus α for each of the individual years. A Pearson's rank correlation shows that α is anti-correlated with the optical-continuum luminosity with slope −0.65 at better than 3σ, strongly suggesting that the continuum luminosity

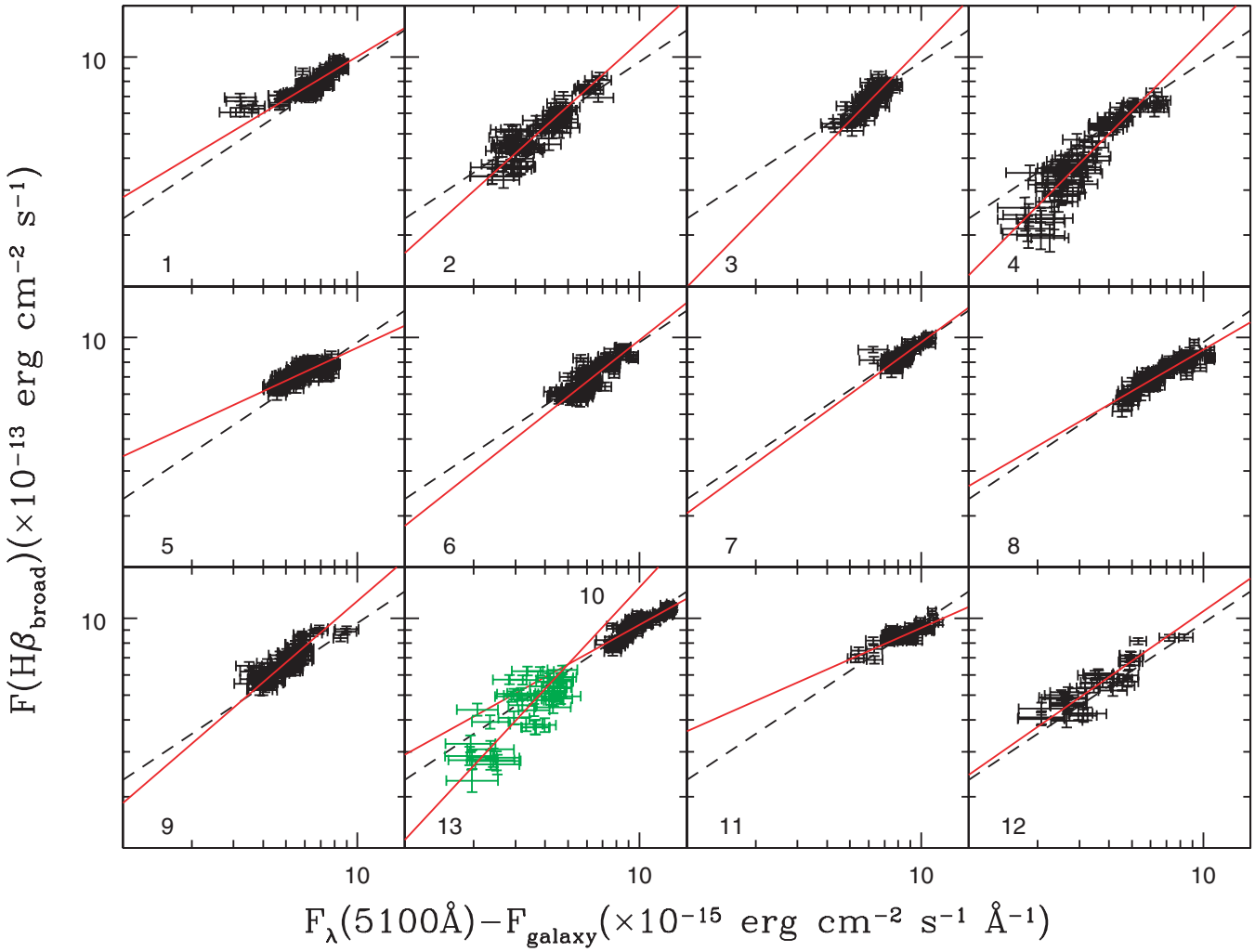

Figure 5. Best-fitting line responsivities, α, for each of the 13 yr of optical data. To guide the eye, we also show the best-fitting line responsivity (dashed line) for the complete data set. For ease of display, panel 10 contains fits to year 10 and year 13.

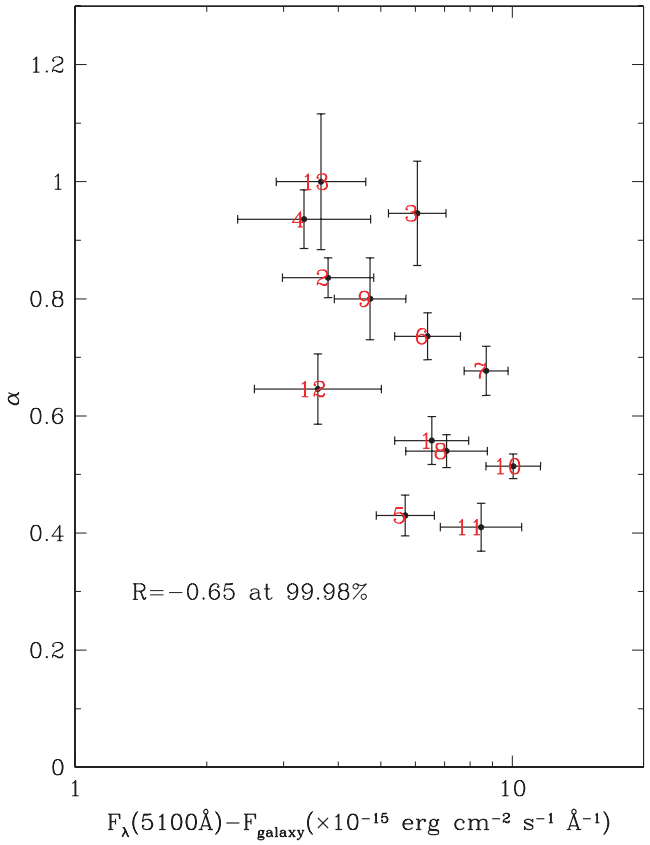

Figure 6. The measured correlation between the line responsivity α, and continuum flux. The numbers indicate the corresponding observing season. A Pearson's rank correlation shows that α is anticorrelated with continuum flux at better than 3σ.

and Hβ line responsivity are intimately connected. Further corroborating evidence for such a relation can be seen in panel 4 of Fig. 5. Season 4 displays the largest range in continuum variation of any of the 13 seasons. It also shows a marked increase in slope with decreasing continuum level. A similar trend, although not as notable, is also seen in year 2. Such short time-scale variations in the line responsivity are unlikely to be due to dynamical effects within the BLR. The dynamical time-scale $\tau_{\rm dyn}$ for the BLR is given by $\tau_{\rm dyn} \approx R/v_{\rm fwhm}$, where R is the luminosity-weighted 'size' of the BLR, and $v_{\rm fwhm}$ is the full width at half-maximum (FWHM) of the rms emission-line profile. Adopting the mean BLR size of $\sim$20 light days and mean FWHM of the Hβ profile of $\sim$5000 km s^{-1}, $\tau_{\rm dyn} \approx$ 3 yr for this source, far longer than any single observing season.

Given the relatively short time-scales over which changes in the emission-line responsivity occur, our preferred interpretation is that variations in α are likely related to changes in continuum flux only. Although there are clearly points which do not obey this general trend (for example, year 7), we suspect that this merely reflects our inability to account for reverberation effects adequately within the spatially extended BLR.[1] For example, we expect the largest discrepancies from the overall trend in Fig. 6 whenever a low continuum state directly follows a high one. This is due to a residual contribution to the overall response in the low state from emission-line gas in the outer BLR. The time delay associated with this region is longer than the luminosity-weighted average, so it may still be responding to the prior high-state continuum flux. Residual reverberation effects such as these most likely account for the comparatively weak response of the line during year 12, a low continuum state which follows two previous high continuum states (years 10 and 11).

We note that the measured line responsivities presented here indicate the relationship between the integrated Hβ emission-line flux and λ5100 Å continuum flux. However, to ascertain the mechanism behind this relation, it is necessary to relate the emission-line flux to the ionizing continuum flux. Because we cannot observe the ionizing continuum directly, we adopt the λ1350 Å continuum flux as a reasonable surrogate. Contemporaneous UV/optical-continuum data (Gilbert & Peterson 2003) reveal a relationship of the form

$$F(\lambda 5100\,\text{Å}) \propto F(\lambda 1350)^{2/3}. \quad (8)$$

Thus the slopes relative to the driving ionizing continuum may be up to a factor of 2/3 smaller than those presented here, ranging from $\sim$0.27 at high continuum flux levels to $\sim$0.67 at low-continuum-flux levels.

An enhanced line response at low incident continuum levels and a reduced line response at high continuum levels matches well the predicted temporal behaviour of the optical recombination lines in recent detailed photoionization calculations of the BLR in NGC 5548 (Korista & Goad 2004). The origin of this behaviour is thought to arise from the strong dependence of the emissivities of these lines on the incident ionizing photon flux, which results in a marked reduction in their responsivity with decreasing distance from the central ionizing continuum source. Their responsivities should therefore display temporal variations due to large changes in the continuum luminosity, with their responsivities expected to be anticorrelated with the continuum level. This is in stark contrast to the behaviour of the high ionization lines (HILs), the line responsivities of which are more strongly correlated with the overall ionization state of the gas than on the incident ionizing continuum flux. Because the line responsivity α is on average smaller for the optical recombination lines than for the HILs, we expect a stronger intrinsic Baldwin effect for these lines than for the HILs, as is generally observed (see, for example, Krolik et al. 1991; Pogge & Peterson 1992; Dietrich et al. 2003).

5 CONCLUSIONS

Our analysis of $\sim$13 yr of optical-continuum and Hβ emission-line data for NGC 5548 shows that the Hβ emission-line responsivity, and hence the slope of the intrinsic Baldwin effect β, displays significant variation on time-scales $\sim$1 yr. The line responsivity is generally anticorrelated with continuum level such that in high continuum states, the emission-line response is weaker on average. Conversely, in low continuum states, the responsivity is stronger than on average. This behaviour is consistent with predictions of photoionization models.

ACKNOWLEDGMENTS

We would like to thank the referee, Ari Laor, for helpful comments leading to clarification of the key points presented in this work. MRG would also like to thank the generous hospitality of the family Korista during the initial stages of this work.

REFERENCES

Baldwin J., 1977, ApJ, 214, 679
Dietrich M., Hamann F., Shields J. C., Constantin A., Heidt J., Jäger K., Vestergaard M., Wagner S. J., 2003, ApJ, 589, 722

[1] The lag is a one number estimate of the luminosity-weighted 'size' of a region which is spatially extended.

Gilbert K. M., Peterson B. M., 2003, ApJ, 587, 123
Goad M. R., 1995, PhD thesis University College London
Kawaguchi T., Mineshige S., Umemura M., Turner E. L., 1998, ApJ, 504, 671
Kinney A. L., Rivolo A. R., Koratkar A. P., 1990, ApJ, 357, 338
Korista K. T., Goad M. R., 2004, ApJ, in press
Korista K. T., Baldwin J. A., Ferland G. J., 1998, ApJ, 507, 24
Krolik J. H., Horne K., Kallman T. R., Malkan M. A., Edelson R. A., Kriss G. A., 1991 ApJ, 371, 541
O'Brien P. T., Goad M. R., Gondhalekar P. M., 1995, MNRAS, 275, 1125
Osmer P. S., Porter A. C., Green R. F., 1994, ApJ, 436, 678
Paltani S., 1999, in Takalo L., Sillanpaa A., eds, ASP Conf. Proc. Vol. 5, BL Lac Phenomenon. Astron. Soc. Pac., San Francisco, 159, 293
Peterson B. M. et al., 2002, ApJ, 581, 197
Pogge R. W., Peterson B. M., 1992, AJ, 103, 1084
Romanishin W. et al., 1995, ApJ, 455, 516

This paper has been typeset from a TEX/LATEX file prepared by the author.